ORGANOMETALLICS

Subscriber access provided by American Chemical Society

Article

# Density Functional Study of Ethylene–Norbornene Copolymerization via Metallocene and Constrained-Geometry Catalysts

Eung-Gun Kim, and Michael L. Klein

*Organometallics*, **2004**, 23 (13), 3319-3326 • DOI: 10.1021/om034136s

**Downloaded from http://pubs.acs.org on December 12, 2008**

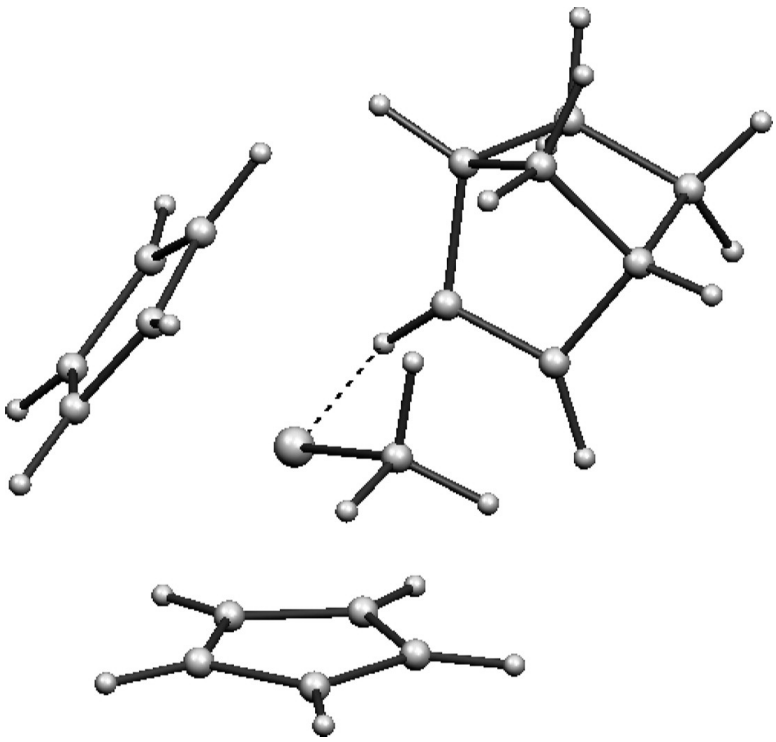

## More About This Article

Additional resources and features associated with this article are available within the HTML version:

- Supporting Information
- Links to the 2 articles that cite this article, as of the time of this article download
- Access to high resolution figures
- Links to articles and content related to this article
- Copyright permission to reproduce figures and/or text from this article

ACS Publications
High quality. High impact.

Organometallics is published by the American Chemical Society. 1155 Sixteenth Street N.W., Washington, DC 20036

ORGANOMETALLICS

Subscriber access provided by American Chemical Society

View the Full Text HTML

ACS Publications
High quality. High impact.

Organometallics is published by the American Chemical Society. 1155 Sixteenth Street N.W., Washington, DC 20036

# Density Functional Study of Ethylene−Norbornene Copolymerization via Metallocene and Constrained-Geometry Catalysts

Eung-Gun Kim* and Michael L. Klein

*Center for Molecular Modeling and Department of Chemistry, University of Pennsylvania, Philadelphia, Pennsylvania 19104-6323*

*Received August 28, 2003*

Single-site Ziegler−Natta catalysts allow a sterically distinct norbornene to copolymerize with ethylene. By performing density functional calculations on $Cp_2ZrCH_3^+$ and $H_2Si(CpNH)$-$ZrCH_3^+$, each representing metallocene and constrained-geometry catalysts (CGC), we have uncovered how the bulky norbornene competes with ethylene for the metal center during the insertion process. Instead of acting as a steric barrier to insertion, the cyclopentyl group of norbornene provides additional agostic sites and disposable ring strain, by which the monomer achieves its high reactivity at low temperature. This effect becomes more pronounced on the less sterically hindered catalyst, leading to a more discriminating catalytic activity of CGC toward the two monomers. The unfavorable endo orientation for insertion of norbornene results from a steric interaction of its bulky ethylene bridge facing the catalyst. A small geometric difference, as exemplified in a structurally similar bicyclooctene, can greatly affect the agosticity, steric hindrance, and ring strain of a cycloolefin.

## Introduction

The discovery and development of homogeneous single-site Ziegler−Natta catalysts have led to improved control over structures of existing polymers and provided tools to design polymers with new architectures. In addition to narrowing the molecular weight distribution and enhancing stereo- and regioselectivity, the new generation of catalysts has made it possible to copolymerize monomers that otherwise could not form a copolymer due to their distinct reactivity ratios. Among those examples is the copolymerization of ethylene with cycloolefins.[1,2,3a,b] In particular, the ethylene−norbornene copolymerization is one of the most studied in terms of kinetics[1,2,3a,b,4a,5] and microstructure of the resulting copolymers.[1,2b,3b−e,4] Now available as a commercial product,[6] ethylene−norbornene copolymers offer high glass transition temperature, high thermal stability, low birefringence, high clarity, and high moisture resistance, some of which are desirable in applications such as optical media and pharmaceutical packaging.

Although systematic experimental studies on metallocene and constrained-geometry catalysts have allowed the identification of governing factors of the associated reaction in each catalyst group,[2b−d,3a,b] fundamental issues remain to be answered and some experimental observations seem even contradictory. For instance, how does a sterically unfavorable norbornene compete with ethylene in the monomer insertion process, or how can the content of norbornene in a copolymer sometimes exceed that of ethylene?[1,2b,c] What dictates the dominance of exo over endo configuration for a norbornene residue in the resulting copolymer[1,4b,7] (see Scheme 1)?

To this end, we explore the insertion mechanism of norbornene and ethylene on two catalysts in their active form, $Cp_2ZrCH_3^+$ and $H_2Si(CpNH)ZrCH_3^+$, representing metallocene (MC) and constrained-geometry catalysts (CGC), respectively, by performing quantum-chemical electronic structure calculations. Starting with the resulting structures from these calculations, we further consider monomer insertion on MC with a norbornene residue as the chain end. We also investigate a structurally similar bicyclo[2.2.2]oct-2-ene (Scheme 1) to address the effect of ring strain.

## Computation

Reaction energy profiles were obtained by following the well-established Cossée−Arlman[8] or Brookhart−Green mechanism[9] for monomer insertion in MC- and CGC-catalyzed polymeri-

* To whom correspondence should be addressed. Current address: School of Chemistry and Biochemistry, Georgia Institute of Technology, Atlanta, Georgia 30332.

(1) Kaminsky, W.; Bark, A.; Arndt, M. *Makromol. Chem., Macromol. Symp.* **1991**, *47*, 83.

(2) (a) Ruchatz, D.; Fink, G. *Macromolecules* **1998**, *31*, 4669. (b) *Macromolecules* **1998**, *31*, 4674. (c) *Macromolecules* **1998**, *31*, 4681. (d) *Macromolecules* **1998**, *31*, 4684.

(3) (a) Thorshaug, K.; Mendichi, R.; Boggioni, L.; Tritto, I.; Trinkle, S.; Friedrich, C.; Mülhaupt, R. *Macromolecules* **2002**, *35*, 2903. (b) Tritto, I.; Boggioni, L.; Jansen, J. C.; Thorshaug, K.; Sacchi, M. C.; Ferro, D. R. *Macromolecules* **2002**, *35*, 616. (c) Provasoli, A.; Ferro, D. R.; Tritto, I.; Boggioni, L. *Macromolecules* **1999**, *32*, 6697. (d) Tritto, I.; Marestin, C.; Boggioni, L.; Zetta, L.; Provasoli, A.; Ferro, D. R. *Macromolecules* **2000**, *33*, 8931. (e) Tritto, I.; Marestin, C.; Boggioni, L.; Sacchi, M. C.; Brintzinger, H.-H.; Ferro, D. R. *Macromolecules* **2001**, *34*, 5770.

(4) (a) Bergström, C. H.; Väänänen, T. L. J.; Seppälä, J. V. *J. Appl. Polym. Sci.* **1997**, *63*, 1071. (b) Bergström, C. H.; Sperlich, B. R.; Ruotoistenmäki, J.; Seppälä, J. V. *J. Polym. Sci. A: Polym. Chem.* **1998**, *36*, 1633.

(5) Park, S. Y.; Choi, K. Y.; Song, K. H.; Jeong, B. G. *Macromolecules* **2003**, *36*, 4216.

(6) *Mod. Plast.* **1995**, *72*, 137.

(7) Arndt, M.; Engehausen, R.; Kaminsky, W.; Zoumis, K. *J. Mol. Catal. A: Chem.* **1995**, *101*, 171.

(8) Cossee, P. *J. Catal.* **1964**, *3*, 80.

(9) Brookhart, M.; Green, M. L. H. *J. Organomet. Chem.* **1983**, *250*, 395.

10.1021/om034136s CCC: $27.50 © 2004 American Chemical Society
Publication on Web 05/18/2004

**Scheme 1. Copolymerization Mechanism of Ethylene and Norbornene in the Presence of a Metallocene Catalyst According to the Cossée−Arlman or Brookhart−Green Mechanism[a]**

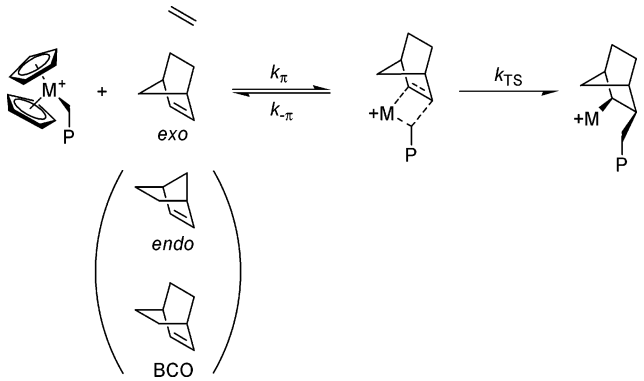


[a] The ligands of the catalyst are not shown in the $\pi$-complex and product for clarity. There are two possible insertion orientations, exo and endo, for a norbornene monomer. Also shown here is bicyclo[2.2.2]oct-2-ene (BCO).

zation. Numerous computational studies of ethylene in these systems exist in the literature.[10−12] Geometry optimizations and energy calculations were performed using a density functional theory (DFT) method with the B3LYP hybrid exchange-correlation functional. The LANL2DZ basis set was used for all atoms.[13] In this double-$\zeta$ quality basis set, the core orbitals are replaced by an effective core potential (1s for C and N; 1s, 2s for Si; 1s, 2s, 2p, 3s, 3p, 3d for Zr). All calculations were carried out using GAUSSIAN 98.[16]

## Results and Discussion

**Norbornene Competing with Ethylene.** An experimental value of the monomer reactivity ratio $r_1$ in the presence of a bridged zirconocene, $MeCHCp_2ZrCl_2$, suggests[2c] that the catalyst can be more favorable toward norbornene (N) than ethylene (E) when the growing chain end is an ethylene residue ($r_1 = k_{EE}/k_{EN} = 0.83$ at 70 °C in toluene, where $k_{mn}$ is the rate constant of insertion of monomer n when the chain end is a residue of monomer m). A question arises: what makes this bulky cycloolefin so competitive with ethylene in copolymerization? The answer does not seem obvious from comparison of the calculated reaction profiles between ethylene and NB-*exo* (norbornene facing *exo* to the catalyst) on MC (see Table 1 and Figure 1).

**Table 1. Energetics of the Insertion Reaction for Ethylene, Norbornene (NB), and Bicyclo[2.2.2]oct-2-ene (BCO) on $Cp_2ZrCH_3^+$ (MC) and $H_2Si(CpNH)ZrCH_3^+$ (CGC)[a]**

| | MC | | | CGC | | |
|---|---|---|---|---|---|---|
| monomer | $\Delta E_b$ | $\Delta E_a$ | $\Delta E_i$ | $\Delta E_b$ | $\Delta E_a$ | $\Delta E_i$ |
| ethylene | −18.31 | 7.46 | −25.48 ($\gamma$)<br>−29.27 ($\beta$) | −26.73 | 9.79 | |
| NB-*exo* | −24.34 | 12.31 | −26.85 ($\gamma$)<br>−22.26 ($\beta'$) | −35.74 | 13.04 | −36.89 ($\gamma$)<br>−31.35 ($\beta'\gamma'$) |
| NB-*endo* | −18.30 | 17.93 | | −30.24 | 16.65 | −33.83 ($\gamma$)<br>−33.73 ($\beta'\gamma'$) |
| BCO | −21.19 | | | −33.63 | 17.03 | −29.80 ($\gamma$)<br>−27.96 ($\beta'\gamma'$) |

[a] Energy changes are given in kcal/mol. $\Delta E_b$ = (energy of the $\pi$-complex, $E_\pi$) − (energy of the reactants, $E_r$); $\Delta E_a$ = (energy of the transition state) − $E_\pi$; $\Delta E_i$ = (energy of the product) − $E_r$.

For a consecutive reaction as seen in metallocene catalysis, where the intermediate attains a preequilibrium with the reactants, the overall rate law is second-order with rate constant $k_2$ written as[17]

$$k_2 = k_{TS}k_\pi/(k_{-\pi} + k_{TS}) \quad (1)$$

where $k_\pi$ and $k_{-\pi}$ are the rate constants for the forward and reverse reactions of equilibrium and $k_{TS}$ for the final step (Scheme 1). Here $k_\pi$ depends mainly on monomer diffusion, because the $\pi$-complex formation is not an activated process. In an equimolar system, $k_\pi{}^E \approx k_\pi{}^N$ and thus $k_2{}^E/k_2{}^N$ becomes

$$\frac{k_2{}^E}{k_2{}^N} \approx \frac{1 + k_{-\pi}{}^N/k_{TS}{}^N}{1 + k_{-\pi}{}^E/k_{TS}{}^E} = \frac{1 + \exp[-(\Delta G_{-\pi}{}^N - \Delta G_{TS}{}^N)/RT]}{1 + \exp[-(\Delta G_{-\pi}{}^E - \Delta G_{TS}{}^E)/RT]} \quad (2)$$

where $\Delta G$ is the free energy change in each step and may be estimated from a vibrational analysis following the standard textbook procedure.[18] From eq 2, we find that the rate constant ratio $k_2{}^E/k_2{}^N$ is determined solely by the free energy barrier differences of the two comonomers. Figure 2 shows calculated values of $\Delta G_{-\pi}$ and $\Delta G_{TS}$ and their difference at various temperatures. $k_2{}^N$ is indeed larger than $k_2{}^E$ at low temperature; that is, norbornene is more reactive than ethylene. $k_2{}^E/k_2{}^N$ rises above unity with increasing temperature, and the faster lowering of $\Delta G_{-\pi}{}^N$ as compared to $\Delta G_{-\pi}{}^E$ contributes

(10) (a) Kawamura-Kuribayashi, H.; Koga, N.; Morokuma, K. *J. Am. Chem. Soc.* **1992**, *114*, 8687. (b) Yoshida, T.; Koga, N.; Morokuma, K. *Organometallics* **1996**, *15*, 766.

(11) (a) Cavallo, L.; Guerra, G. *Macromolecules* **1996**, *29*, 2729. (b) Iarlori, S.; Buda, F.; Meier, R. J.; van Doremaele, G. H. J. *Mol. Phys.* **1996**, *87*, 801.

(12) (a) Woo, T. K.; Fan, L.; Ziegler, T. *Organometallics* **1994**, *13*, 2252. (b) Fan, L.; Harrison, D.; Woo, T. K.; Ziegler, T. *Organometallics* **1995**, *14*, 2018. (c) Lohrenz, J. C. W.; Woo, T. K.; Ziegler, T. *J. Am. Chem. Soc.* **1995**, *117*, 12793. (d) Lohrenz, J. C. W.; Woo, T. K.; Fan, L.; Ziegler, T. *J. Organomet. Chem.* **1995**, *497*, 91. (e) Margl, P.; Lohrenz, J. C. W.; Ziegler, T.; Blöchl, P. E. *J. Am. Chem. Soc.* **1996**, *118*, 4434.

(13) The LANL2DZbasis set[14] was designed for transition-metal elements such as Zr. The Gaussian implementation of LANL2DZ uses D95V (Dunning/Huzinaga valence double-$\zeta$[15]) for H, C, N, and Si. Calculations were also performed by using the minimal STO-3G for the atoms in the ligands and 3-21G for those involved in the reaction (the chain end and monomers), as done similarly by Morokuma and co-workers in their ab initio studies of ethylene and propylene on zirconocene catalysts.[10] Mixing the basis sets of different levels was found to affect the charge distribution and geometry around the metal center and Cp ligands; in the bare $Cp_2ZrCH_3^+$, for instance, the metal charge was 0.617 (0.833 with LANL2DZ) and the metal−Cp distance was 2.217 (2.233) Å. However, the conclusions of the study remained unaffected, indicative of the minor role played by the spectator ligands in the copolymerization reaction.

(14) Hay, P. J.; Wadt, W. R. *J. Chem. Phys.* **1985**, *82*, 299.

(15) Dunning, T. H., Jr.; Hay, P. J. In *Modern Theoretical Chemistry*; Schaefer, H. F., III, Ed.; Plenum: New York, 1976; Vol. 3, pp 1−28.

(16) Frisch, M. J.; Trucks, G. W.; Schlegel, H. B.; Scuseria, G. E.; Robb, M. A.; Cheeseman, J. R.; Zakrzewski, V. G.; Montgomery, J. A., Jr.; Stratmann, R. E.; Burant, J. C.; Dapprich, S.; Millam, J. M.; Daniels, A. D.; Kudin, K. N.; Strain, M. C.; Farkas, O.; Tomasi, J.; Barone, V.; Cossi, M.; Cammi, R.; Mennucci, B.; Pomelli, C.; Adamo, C.; Clifford, S.; Ochterski, J.; Petersson, G. A.; Ayala, P. Y.; Cui, Q.; Morokuma, K.; Malick, D. K.; Rabuck, A. D.; Raghavachari, K.; Foresman, J. B.; Cioslowski, J.; Ortiz, J. V.; Stefanov, B. B.; Liu, G.; Liashenko, A.; Piskorz, P.; Komaromi, I.; Gomperts, R.; Martin, R. L.; Fox, D. J.; Keith, T.; Al-Laham, M. A.; Peng, C. Y.; Nanayakkara, A.; Gonzalez, C.; Challacombe, M.; Gill, P. M. W.; Johnson, B. G.; Chen, W.; Wong, M. W.; Andres, J. L.; Head-Gordon, M.; Replogle, E. S.; Pople, J. A. *Gaussian 98*; Gaussian, Inc.: Pittsburgh, PA, 1998.

(17) Atkins, P. W. *Physical Chemistry*, 2nd ed.; Oxford University Press: Oxford, U.K., 1982.

(18) McQuarrie, D. A. *Statistical Mechanics*; Harper Collins: New York, 1976.

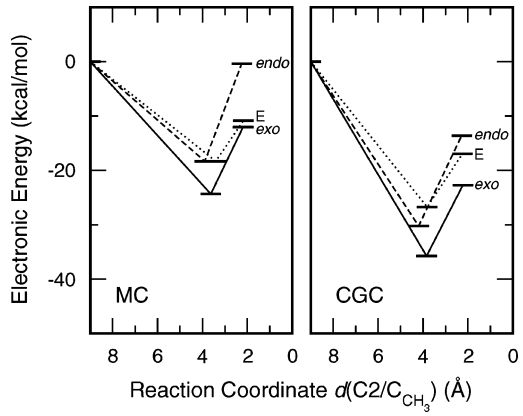


**Figure 1.** Energy profiles of insertion for ethylene and norbornene on MC and CGC.

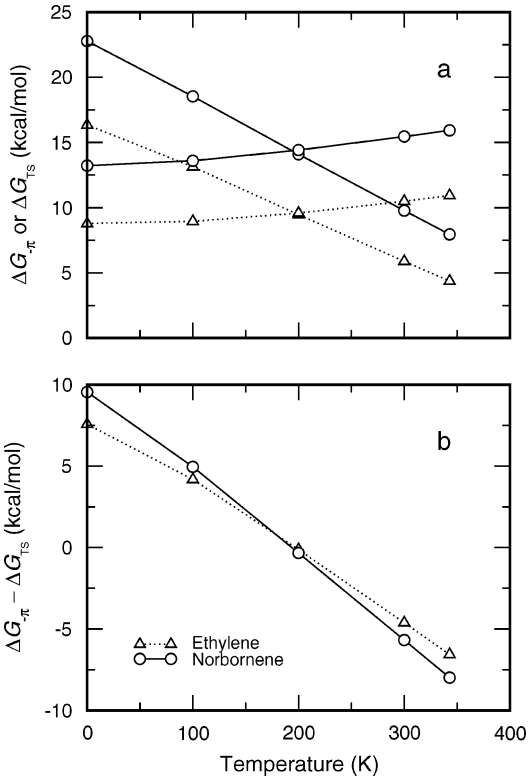


**Figure 2.** Temperature dependence of (a) the free energy barriers for the backward ($\Delta G_{-\pi}$) and forward ($\Delta G_{TS}$) reactions of the $\pi$-complex and (b) their difference. The latter can be used to predict the relative reactivity of ethylene and norbornene.

to the reversal of the rate constants. Similar behavior is observed on CGC; in this case $k_2^N$ and $k_2^E$ are so different from each other that their relative magnitudes reverse at a higher temperature.

We note that a change in the free energy barrier with temperature is mainly entropic. When the monomer and catalyst are brought together to become unimolecular, the number of interaction pairs increases. The formation of "bonds" between these pairs, whether attractive or repulsive in nature, reduces the degrees of freedom in the resulting species. As will be seen below, norbornene forms an extra number of interaction pairs in comparison with ethylene. Therefore, an entropic loss upon complex formation is more dramatic with norbornene than with ethylene. The calculated temperature dependence of the monomer reactivity ratio is also consistent

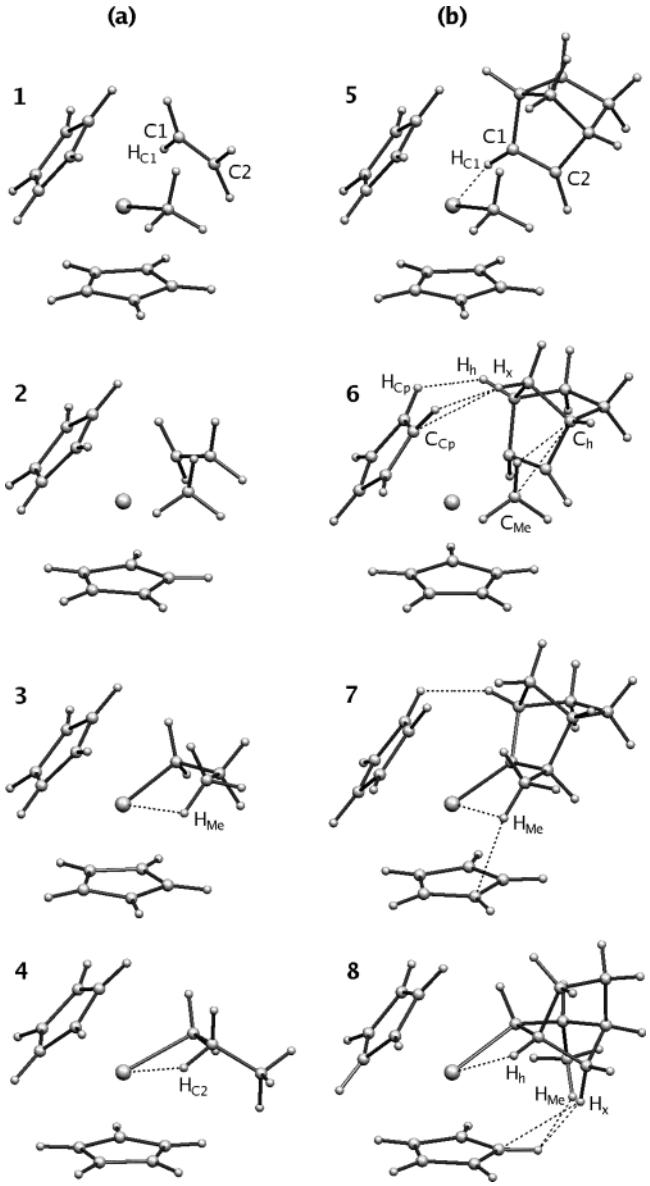


**Figure 3.** Optimized structures of (a) ethylene-MC and (b) NB-*exo*-MC: the $\pi$-complexes (**1**, **5**), the transition states (**2**, **6**), and the products in $\gamma$- (**3**, **7**) and $\beta$- (**4**)/$\beta'$-agostic (**8**) conformation. Note that the $\beta'$-agostic interaction seen in **8** is with a bridgehead hydrogen atom $H_h$. Pairs of atoms interacting sterically and/or agostically are shown as connected by dotted lines. In **1,** $d$(C1/Zr) = 2.913, $d$(C2/Zr) = 2.887, and $d(H_{C1}/Zr)$ = 3.243. In **5**, $d$(C1/Zr) = 2.691, $d$(C2/Zr) = 3.110, and $d(H_{C1}/Zr)$ = 2.712. In **6**, $d(H_h/H_{Cp})$ = 2.233, $d(H_x/H_{Cp})$ = 2.232, $d(H_x/C_{Cp})$ = 2.657, $d(C_h/C_{Me})$ = 2.906, and $d(C_h/H_{Me})$ = 2.716. In **3**, $d(H_{Me}/Zr)$ = 2.320. In **7**, $d(H_h/H_{Cp})$ = 2.215, $d(H_{Me}/C_{Cp})$ = 2.705, and $d(H_{Me}/Zr)$ = 2.295. In **4**, $d(H_{C2}/Zr)$ = 2.164. In **8**, $d(H_h/Zr)$ = 2.355, $d(H_{Me}/H_{Cp})$ = 2.114, $d(H_x/H_{Cp})$ = 2.867, and $d(H_x/C_{Cp})$ = 2.724. Here $d$ is the interatomic distance in Å.

with experimental observations of an increase in the norbornene content with decreasing copolymeriztion temperature.[4a]

Figure 3 shows a series of optimized structures of ethylene and NB-*exo* on MC (NB-*exo*-MC) at different stages of monomer insertion. The bulkiness of the cyclic group of NB—if one views NB as an ethylene derivative substituted with a cyclopentyl ring—prevents a close placement of the C=C $\pi$-electrons near Zr during the

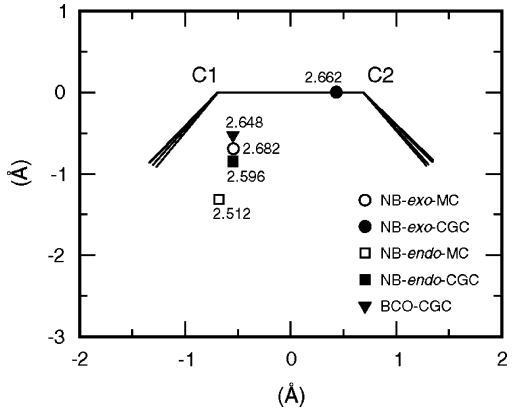


**Figure 4.** Locations of Zr from different $\pi$-complexes projected onto their respective HC═CH planes. The HC═CH groups are denoted by doubly bent solid lines superimposed on one another. A number accompanying each symbol denotes the distance between Zr and the plane. In the case of ethylene-MC, the projected Zr is found right on C═C at the center (not shown). As the projected Zr moves away from C═C in the plane, the binding becomes weak (see Table 1 for binding energies).

$\pi$-complex formation. As a result, the C═C plane is tilted from the orientation assumed by ethylene (see Figure 4 for the projection of Zr onto the C═C plane). However, this tilting seems to work toward enhancing the binding, because it places C1 and its pendant hydrogen atom $H_{C1}$ closer to Zr than those of ethylene; the closer C1 gains an electrostatic interaction with the positively charged Zr, and the $H_{C1}$ forms an agostic interaction. The latter effect is manifested in an elongated C1−$H_{C1}$ bond of 1.095 Å (1.086 Å before complex formation). Steric overlap becomes severe in the transition state and raises the activation barrier; the bridgehead and methylene bridge interact strongly with the Cp ligand and methyl group.

**Catalytic Activity toward Norbornene: Metallocene vs Constrained-Geometry Catalysts.** Although CGC is sterically less congested and thus its metal center is more accessible than its counterpart with two Cp rings, CGC is generally less active than MC toward simple olefin monomers such as ethylene and propylene. In their comparative computational study, Ziegler and co-workers[12a] have shown that the less congestive environment, along with a more positive charge of the metal, allows a tighter binding between ethylene and the metal center, which raises the transition state energy. Recent experimental studies on ethylene−norbornene copolymerization[2b−d] suggest that the same argument may apply to the case of norbornene, and our calculated energetics also seem to support this idea.

In comparing the calculated reaction profiles of ethylene and norbornene in Figure 1, we note that they are more distinct from each other on CGC than on MC; for instance, the difference in binding energy $E_b$ between ethylene and NB-*exo* increases from 6.03 to 9.01 kcal/mol in going from MC to CGC (Table 1). This is not well explained by the steric argument, according to which the less sterically hindered CGC should be less discriminating toward the bulky norbornene and ethylene. In this section, we discuss what makes the discrimination pronounced on CGC.

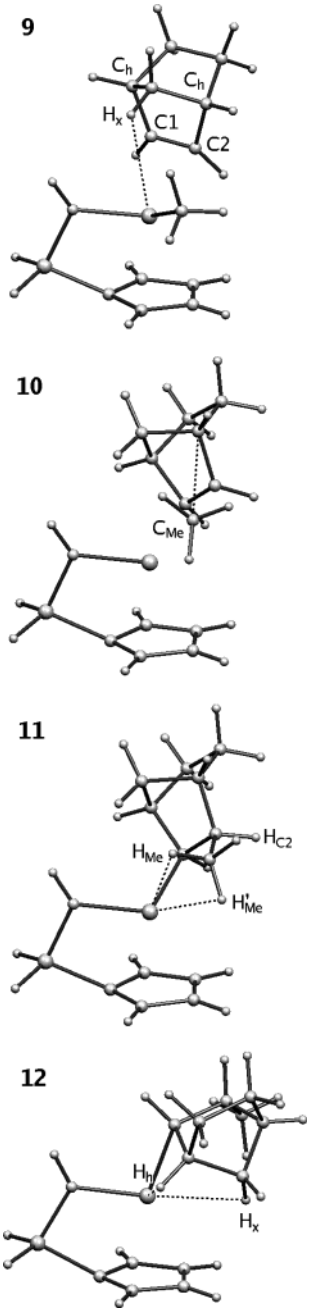


**Figure 5.** Optimized structures of NB-*exo*-CGC: the $\pi$-complex (**9**), the transition state (**10**), and the product in $\gamma$- (**11**) and $\beta'\gamma'$-agostic (**12**) conformation. In **9**, $d(H_x/Zr)$ = 2.791, $l(C-H_x)$ = 1.102 (1.095 without agosticity), $\angle C_hC1C2$ = 108.0, and $\angle C1C2C_h$ = 106.5. In **10**, $d(C_h/C_{Me})$ = 2.901, $\angle C_hC1C2$ = 104.6, and $\angle C1C2C_h$ = 106.8. In **11**, $d(H_{Me}/Zr)$ = 2.517, $d(H'_{Me}/Zr)$ = 2.425, $\angle C_hC1C2$ = 103.0, and $\angle C1C2C_h$ = 101.6. In **12**, $d(H_h/Zr)$ = 2.433 and $d(H_x/Zr)$ = 2.736. Here $d$ is the interatomic distance in Å, $l$ is the bond length in Å, and $\angle$ is the bond angle in deg.

The $\pi$-complex structure **9**, given in Figure 5, shows that the absence of one Cp ligand restores the orientation of the C═C plane relative to Zr (see also Figure 4 for a new location of Zr). Building on the renewed C═C/Zr interaction, norbornene further strengthens the binding through an agostic hydrogen atom $H_x$ on the methylene bridge. The agostic enhancement accounts for much of the observed excess binding energy of norbornene on CGC.

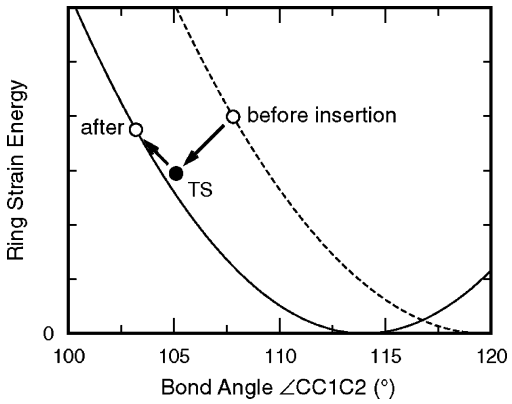


**Figure 6.** Schematic of the change in the ring strain level of norbornene during rehybridization.

In approaching the transition state, **10**, the agostic interaction at $H_x$ weakens, raising the activation energy. Steric overlap of a bridgehead carbon atom $C_h$ with the methyl group also contributes to the increase. However, the transition state is not destabilized so much as the $\pi$-complex is stabilized, and it remains far below that of ethylene (Figure 1). This calls for a source of stabilization in the transition state. We estimate from a separate calculation[19] that a ring strain energy of about 2.5 kcal/mol is released during insertion (we will come back to this discussion later). The amount of released strain energy seems to fall short to account for the 5.8 kcal/mol gap between norbornene and ethylene. However, we argue that 2.5 kcal/mol only serves as the lower limit of the actual amount released *at the transition state*. During insertion, the geometry of norbornene moves away from the unstrained states of both $sp^2$ and $sp^3$ (see the evolution of $\angle C_hC1C2$ and $\angle C1C2C_h$). This suggests the transition state has a smaller ring strain than the product, as illustrated schematically in Figure 6, because it should be located close to the $sp^3$ potential energy surface. (We recall that the structure of a transition state in general resembles that of the product.) The similar transition state energy levels of norbornene and ethylene on MC may be understood in the same context. In this case, stabilization by the ring strain release is compromised by a strong steric interaction with the catalyst.

Comparison of the relative stabilities between different conformations of the norbornene residue in the product (see Table 1) indicates that immediate or $\gamma$-agostic conformations are more favorable than secondary conformations, unlike the case of ethylene. The dangling hydrogen atoms on the nonrotatable C1−C2 bond in the norbornene residue face away from the metal center (see **7**, **8**, **11**, and **12**). This configuration disallows $H_{C2}$ to form a $\beta$-agostic pair with Zr, the key interaction pair for an ethylene residue to obtain the lowest energy conformation. The absence of a $\beta$-agostic conformation also sets apart norbornene from ethylene and other acyclic olefin monomers in polymerization kinetics because $\beta$-hydride elimination and H-transfer to a monomer,[12d] both of which require the $\beta$-agostic conformation as a precursor, are no longer possible chain transfer mechanisms. A reduced number of pathways for the chain transfer may explain an increasing degree of polymerization by MC derivatives[2d] and the appearance of a quasi-living character by CGC,[3a] with increasing norbornene concentration in the feed; the opposite is observed with comonomers such as 1-hexene and 1-octene.[20]

Another product characteristic shared by MC and CGC toward norbornene is an agostic interaction at a bridgehead hydrogen atom $H_h$ in the secondary conformation (see **8** and **12**). This type of $\beta$-agostic interaction should not be seen as a possible precursor to $\beta$-hydride elimination, because an elimination reaction leading to formation of a double bond on a bridgehead carbon atom in a fused-ring system (between $C_h$ and C1 here) is normally not allowed and would violate Bredt's rule.[21] Unlike the bridgehead hydrogen, the methylene bridge hydrogen $H_x$ behaves differently toward MC and CGC: $H_x$ is attractive on CGC but repulsive on MC.

**Exo over Endo.** $^{13}C$ NMR structural analyses of norbornene residues in the copolymer[1] and homooligomer[7] revealed that bond formation occurs exclusively in the exo configuration.[22] Comparison of the calculated energetics between the exo and endo configurations indicates that our model correctly predicts the preferred insertion orientation on both MC and CGC; a smaller binding energy and a higher activation barrier of the endo form make the exo configuration favorable (see Table 1 and Figure 1).

Figure 7 shows the endo insertion on MC. In the $\pi$-complex **13**, the bulkier ethylene bridge tilts the C═C plane similarly as the methylene bridge did in the exo orientation, but the resulting dislocation is so great that the $\pi$-electron donation to Zr may barely exist, as shown in Figure 4. This overshadows a strong agostic gain through $H_{C1}$. In the transition state **14**, steric overlap by the bulky ethylene bridge becomes realized, creating a large energy gap of 11.66 kcal/mol between endo and exo.

In the endo form of the $\pi$-complex with CGC, **15**, shown in Figure 8, an ethylene bridge hydrogen atom $H_{n1}$ serves as an agostic site as a methylene bridge hydrogen atom did in the exo species. The binding energy is, however, smaller than in the exo form. The weaker binding is due to a less open structure of the endo face, which in turn dislocates C═C from Zr, as shown in Figure 4.

As one approaches the transition state in NB-*endo*-CGC (**16**), the agostic ethylene bridge turns steric; one bridge hydrogen atom acts against the NH group and the other against the chain end. The change in the nature of the interaction brings a larger energy change to the system than in the exo orientation, where the agostic site simply disappears.

In the $\beta'\gamma'$-agostic conformation on CGC, the secondary product conformation for both exo (**12**) and endo

(19) The released strain energy was estimated by comparing the hydrogenation reactions of norbornene and ethylene. An eclipsed conformation was used for ethane because the corresponding bond in norbornane is nonrotatable. The same procedure was also used for bicyclooctene.

(20) *Polypropylene and Other Polyolefins*; van der Ven, S., Ed.; Elsevier: Amsterdam, The Netherlands, 1990; p 413.

(21) Sykes, P. *A Guidebook to Mechanism in Organic Chemistry*, 6th ed.; Longman Scientific & Technical: Essex, U.K., 1986; pp 259−260.

(22) The exclusive exo insertion has been reported also in late-transition-metal catalysis. For a recent review on this topic, see: Goodall, B. L. In *Late Transition Metal Polymerization Catalysis*; Rieger, B., Baugh, L. S., Kacker, S., Striegler, S., Eds.; Wiley-VCH: Weinheim, Germany, 2003; pp 101−154.

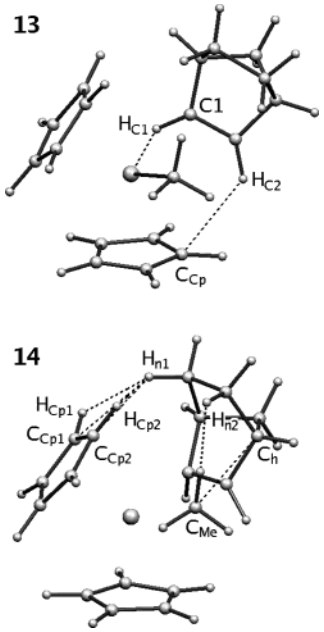


**Figure 7.** Optimized structures of NB-*endo*-MC: the $\pi$-complex (**13**) and the transition state (**14**). In **13**, $d(H_{C1}/Zr) = 2.517$, $l(C1-H_{C1}) = 1.098$, $d(C1/Zr) = 2.737$, and $d(H_{C2}/C_{Cp}) = 2.734$. In **14**, $d(H_{n1}/H_{Cp1}) = 2.139$, $d(H_{n1}/C_{Cp1}) = 2.564$, $d(H_{n1}/H_{Cp2}) = 2.153$, $d(H_{n1}/C_{Cp2}) = 2.571$, $d(H_{n2}/H_{Me}) = 2.000$, and $d(C_h/C_{Me}) = 3.066$. Here $d$ is the interatomic distance in Å and $l$ is the bond length in Å.

forms (**18**), the bridge and bridgehead hydrogen atoms provide an important source of agosticity. The doubly agostic methyl group adds stability to the $\gamma$-agostic conformation of exo (**11**) and endo forms (**17**); one agostic C−H bond promotes the donation of $\sigma$ electrons to Zr by another C−H on the same carbon atom and vice versa.

**Ring Strain.** We argued earlier that the ring strain may be important only in the transition state. To further address its role, we investigated another cycloolefin molecule. Bicyclooctene (BCO), shown in Scheme 1, and norbornene are structurally similar but distinct in contained strain. The same procedure[19] undertaken for norbornene gives BCO an *increase* of the ring strain by 3.29 kcal/mol upon saturation. How will this cycloolefin behave on the catalyst?

Figure 9 shows the insertion energy profile of BCO on CGC, along with those of norbornene in the exo and endo forms on the same catalyst. Comparison of the energy profiles indicates that BCO is more favorable than the similar-faced NB-*endo*. However, an insertion of BCO is unlikely to take place, due to its high activation energy barrier, which is consistent with an experimental observation[23] that BCO is not (co)polymerizable.

During insertion the bond angle $\angle C_hC1C2$ of BCO decreases (see Figure 10), moving away from the equilibrium values of both $sp^2$ and $sp^3$. We recall that a similar behavior was observed with norbornene. However, a significant lowering of the ring strain level in the transition state may not be expected for BCO, because of the elevated ring strain after insertion. The lower transition state of BCO-CGC as compared to that

(23) Arndt, M. Dissertation, Universität Hamburg; Hamburg, Germany, 1993.

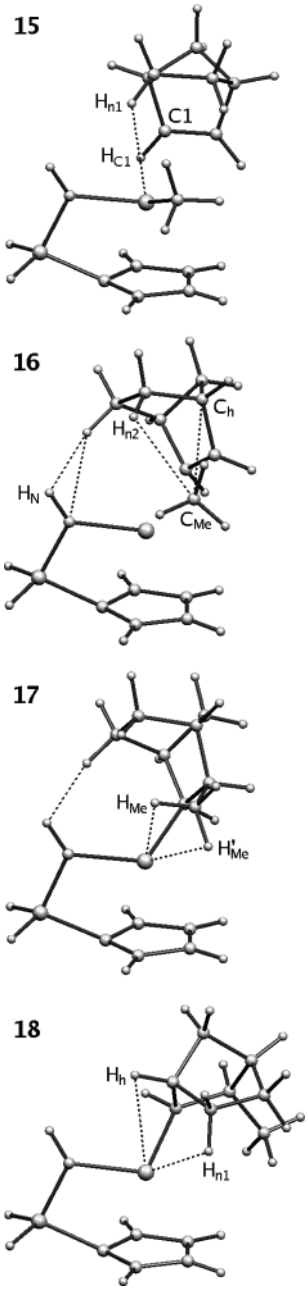


**Figure 8.** Optimized structures of NB-*endo*-CGC: the $\pi$-complex (**15**), the transition state (**16**), and the product in $\gamma$- (**17**) and $\beta'\gamma'$-agostic (**18**) conformation. In **15**, $d(H_{C1}/Zr) = 2.651$, $l(C1-H_{C1}) = 1.093$, and $d(H_{n1}/Zr) = 2.745$. In **16**, $d(H_{n1}/H_N) = 2.287$, $d(H_{n1}/N) = 2.578$, $d(H_{n2}/C_{Me}) = 2.728$, and $d(C_h/C_{Me}) = 3.101$. In **17**, $d(H_{n1}/H_N) = 2.282$, $d(H_{Me}/Zr) = 2.493$, and $d(H'_{Me}/Zr) = 2.452$. In **18**, $d(H_h/Zr) = 2.715$ and $d(H_{n1}/Zr) = 2.297$. Here $d$ is the interatomic distance in Å and $l$ is the bond length in Å.

of NB-*endo* finds a source in reduced steric interactions. Figure 10 shows that BCO **20** does not list the ethylene bridge as a steric site, unlike NB-*endo* **16**. This is due to a slight geometric difference between two cycloolefins. In isolated BCO, the ethylene bridge is located farther away from the C═C bond, whereas two neighboring hydrogen atoms on the bridge, $H_{b1}$ and $H_{b2}$, are closer to each other: that is, $d(C1/H_{b1}) = 2.786$ and $d(H_{b1}/H_{b2}) = 2.341$ in BCO, and $d(C1/H_{n1}) = 2.698$ and $d(H_{n1}/H_{n2}) = 2.415$ for NB.

In the stage of $\pi$-binding, where little or no contribution of the ring strain is expected, the geometric differ-

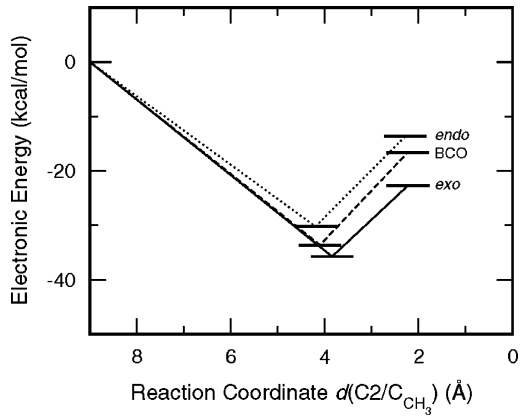


**Figure 9.** Energy profiles of insertion of two possible orientations, exo and endo, for the incoming norbornene monomer. Also shown is the energy profile for BCO, which has two identical orientations similar to endo. All three reactions are catalyzed by CGC.

ence detailed above makes BCO **19** a stronger binder than NB-*endo* **15**. The more open structure of BCO allows the C═C bond to position on Zr better (Figure 4).

The ring strain effect is evident in the product, as expected. Table 1 shows that both $\gamma$- and $\beta'\gamma'$-agostic conformations of BCO-CGC are higher in energy than those of NB-*endo*-CGC, by 4.03 and 5.77 kcal/mol, respectively. Inspection of the conformer structures indicates that BCO (**21** and **22**) and NB-*endo* (**17** and **18**) in the same conformation have very similar interaction pairs. Therefore, their relative stability should come mainly from the ring strain. The energy differences are also consistent with an estimated 5.8 kcal/mol from the model hydrogenation reactions.[19]

**Chain End Effect.** So far our discussion has been built around the very first insertion step by modeling the growing chain end with a methyl group. Although this model serves to capture important aspects of the insertion mechanism beyond the very first event of monomer insertion, its applicability will be limited to a situation where the chain end consists of an ethylene or similar residue. In this section, we present results when the chain end is replaced by a norbornene residue. We used the $\beta'$-agostic conformer of NB-*exo*-MC, **8**, as the catalyst because no $\pi$-complexes were found with the more stable $\gamma$-agostic conformer, **7**, due to the methyl group blocking the coordination site on Zr.

Experiments on kinetics and microstructure have shown that the catalyst inserts ethylene preferentially to norbornene when its chain end is a norbornene residue[3b] and that if the catalyst takes norbornene it prefers the meso to the racemic dyad.[3e] Interpretation of these observations seems straightforward from a steric point of view. Our calculated energy profiles, given in Table 2, show that switching the chain end indeed raises the transition state of norbornene well over that of ethylene and that meso is the favored orientation. However, the overall picture of the calculated energy profiles is far from trivial, especially when it comes to comparing ethylene and norbornene; if we only look at the binding energy, even the racemic orientation of norbornene is favored over ethylene. We also note the transition state *above* the energy level of the reactants

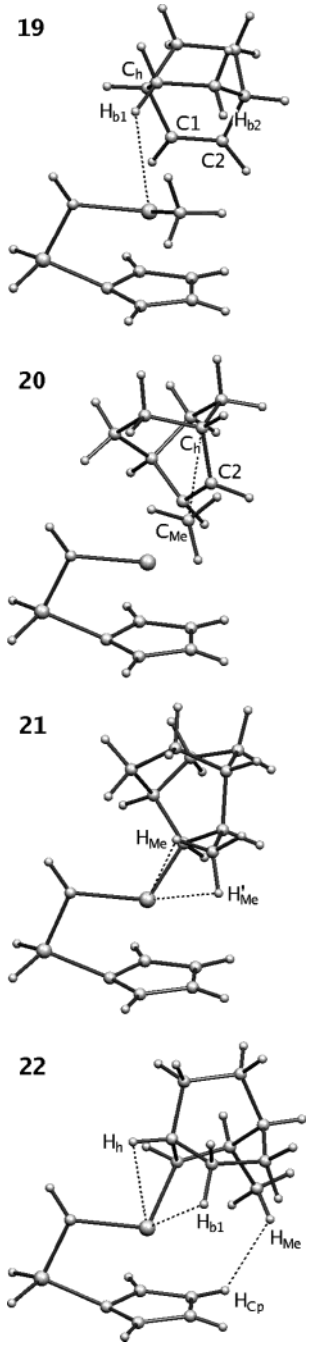


**Figure 10.** Optimized structures of BCO-CGC: the $\pi$-complex (**19**), the transition state (**20**), and the product in $\gamma$- (**21**) and $\beta'\gamma'$-agostic (**22**) conformation. In **19**, $d(H_{b1}/Zr)$ = 2.832 and $\angle C_hC1C2$ = 114.0. In **20**, $d(C_h/C_{Me})$ = 2.949 and $\angle C_hC1C2$ = 111.3. In **21**, $d(H_{Me}/Zr)$ = 2.549, $d(H'_{Me}/Zr)$ = 2.401, and $\angle C_hC1C2$ = 109.3. In **22**, $d(H_h/Zr)$ = 2.457, $d(H_{b1}/Zr)$ = 2.338, and $d(H_{Me}/H_{Cp})$ = 2.253. Here $d$ is the interatomic distance in Å and $\angle$ is the bond angle in deg.

for both monomers. Again, we apply the argument developed earlier to this case. With a larger, negative energy difference between the reactants and transition state for norbornene, it immediately follows from eq 2 that $k_2^E/k_2^N > 1$ at 0 K. Assuming a temperature dependence of the entropic contribution to $\Delta G$ similar to that which we observed with the methyl chain end, we can expect the reactivity ratio to remain above unity at $T > 0$.

**Table 2. Energetics of the Insertion Reaction for Ethylene and Norbornene When the Chain End Is a Norbornene Residue[a]**

| monomer | $\Delta E_b$ | $\Delta E_a$ | $\Delta E_i$ |
|---|---|---|---|
| ethylene | −12.30 | 21.79 | −27.14 ($\gamma$) |
| NB-*meso* | −16.47 | 27.04 | |
| NB-*rac* | −14.25 | | |

[a] The $\beta'$-agostic conformer of NB-*exo*-MC, **8**, was used as the catalyst. Norbornene approaches the catalyst in an exo orientation to form either a meso (NB-*meso*) or racemic (NB-*rac*) dyad. Energy changes are given in kcal/mol.

## Conclusions

We studied the monomer insertion mechanism in single-site Ziegler−Natta copolymerization of ethylene and norbornene, where the two comonomers compete for the catalytic site. By carrying out density functional calculations on model structures of the metallocene and constrained-geometry catalysts, we identified four crucial factors that dictate the associated reactions: agosticity, steric hindrance, entropy, and ring strain. In the design of a new cycloolefin monomer, the first three factors may be realized by introducing the bulkiness and the fourth by containing a disposable ring strain in the structure. It seems that norbornene does an amazing job in optimizing all four factors, because even a small geometrical change could make the molecule no longer useful, as seen in the case of bicyclooctene.

**Acknowledgment.** Part of this work was done when E.G.K. was at LG Chemical Ltd. in Korea.

OM034136S